Variations in soil carbon dioxide efflux across a thaw slump chronosequence in northwestern Alaska

2014 Environ. Res. Lett. 9 025001

(http://iopscience.iop.org/1748-9326/9/2/025001)

OPEN ACCESS
IOP Publishing
Environmental Research Letters
Environ. Res. Lett. **9** (2014) 025001 (11pp)
doi:10.1088/1748-9326/9/2/025001

Variations in soil carbon dioxide efflux across a thaw slump chronosequence in northwestern Alaska

A E Jensen[1], K A Lohse[2], B T Crosby[1] and C I Mora[3]

[1] Department of Geosciences, Idaho State University, Pocatello, ID 83201, USA
[2] Department of Biological Sciences, Idaho State University, Pocatello, ID 83201, USA
[3] Earth and Environmental Science, Los Alamos National Laboratory, Los Alamos, NM 87545, USA

E-mail: aejensen02@gmail.com

Received 12 July 2013, revised 3 January 2014
Accepted for publication 6 January 2014
Published 21 February 2014

Abstract

Warming of the arctic landscape results in permafrost thaw, which causes ground subsidence or thermokarst. Thermokarst formation on hillslopes leads to the formation of thermal erosion features that dramatically alter soil properties and likely affect soil carbon emissions, but such features have received little study in this regard. In order to assess the magnitude and persistence of altered emissions, we use a space-for-time substitution (thaw slump chronosequence) to quantify and compare peak growing season soil carbon dioxide (CO_2) fluxes from undisturbed tundra, active, and stabilized thermal erosion features over two seasons. Measurements of soil temperature and moisture, soil organic matter, and bulk density are used to evaluate the factors controlling soil CO_2 emissions from each of the three chronosequence stages. Soil CO_2 efflux from the active slump is consistently less than half that observed in the undisturbed tundra or stabilized slump (1.8 versus 5.2 g CO_2–C m^{-2} d^{-1} in 2011; 0.9 versus 3.2 g CO_2–C m^{-2} d^{-1} in 2012), despite soil temperatures on the floor of the active slump that are 10–15 °C warmer than the tundra and stabilized slump. Environmental factors such as soil temperature and moisture do not exert a strong control on CO_2 efflux, rather, local soil physical and chemical properties such as soil organic matter and bulk density, are strongly and inversely related among these chronosequence stages ($r^2 = 0.97$), and explain ~50% of the variation in soil CO_2 efflux. Thus, despite profound soil warming and rapid exposure of buried carbon in the active slump, the low organic matter content, lack of stable vegetation, and large increases in the bulk densities in the uppermost portion of active slump soils (up to ~2.2 g^{-1} cm^{-3}) appear to limit CO_2 efflux from the active slump. Future studies should assess seasonal fluxes across these features and determine whether soil CO_2 fluxes from active features with high organic content are similarly low.

Keywords: climate change, CO_2 efflux, arctic, thaw slump, thermokarst, chronosequence, controls on CO_2 efflux, soil temperature, soil moisture, bulk density, soil organic matter, thermal erosion

1. Introduction

Warming of the Arctic permafrost has received international attention and is projected to increase with future changes in climate (Arctic Climate Impact Assessment 2004, Duarte *et al* 2012, IPCC 2007, Winton 2006). This warming has

accelerated widespread permafrost degradation throughout Alaska (Hinzman *et al* 2005, Jorgenson *et al* 2006, 2010, Lawrence *et al* 2008, Rowland *et al* 2010). Progressive permafrost degradation may increase microbial decomposition and soil respiration, releasing greenhouse gases, such as CO_2 and methane (CH_4), to the atmosphere (Natali *et al* 2011, Schuur and Abbott 2011, Schuur *et al* 2008, 2009). The transfer of vast stores of previously frozen carbon from permafrost to the atmosphere may induce positive feedbacks with global climate warming (Koven *et al* 2011, Schuur *et al* 2008); however, the magnitude and timing of carbon release are poorly constrained. To better understand this climate change impact, recent studies examine changes in soil physical properties and hydrology associated with permafrost thaw, how permafrost will thaw across a heterogeneous landscape, as well as the temperature and moisture constraints on the decomposition of previously frozen carbon (Grosse *et al* 2011, Hinzman *et al* 2005, Rowland *et al* 2010, Schuur and Abbott 2011, Schuur *et al* 2008).

A direct consequence of permafrost degradation is thermokarst, where thaw leads to ground subsidence, directly impacting soil and hydrologic properties (Grosse *et al* 2011, Jorgenson *et al* 2008, Rowland *et al* 2010). Thermokarst formed by gradual thaw in regions of low relief and stable topography typically results in increased water storage, increased activity in soil carbon and nutrient pools due to active layer deepening, and changes to vegetation and landscape topography (Jorgenson and Osterkamp 2005, Jorgenson *et al* 2008, Vogel *et al* 2009). Most previous studies of soil carbon dynamics and soil CO_2 efflux in the Arctic have been small in spatial scale ($<10\ m^2$) and conducted in areas of gradual thaw, where active layer thaw deepens into organic-rich substrates and changes the rates and mechanisms of carbon cycling within the ecosystem (Lee *et al* 2011, Schuur *et al* 2009, Vogel *et al* 2009). These studies generally show that CH_4 and/or CO_2 production increases as the thermokarst matures.

In contrast, hillslope thermokarst formation can result in catastrophic slumping and thermal erosion, causing a multitude of cascading effects: detachment and/or erosion of the surface organic horizon, increased exposure of buried soils, increased exposure to incoming solar radiation, extensive and deep cryoturbation, increased erosion by surface overflow, and rapid fluctuations in soil moisture conditions (Gooseff *et al* 2009, Kokelj and Jorgenson 2013). Changes in carbon fluxes from large, rapid thermal erosional features such as retrogressive thaw slumps have received little attention. The increasing recognition of hillslope thermokarst features throughout the Arctic (Gooseff *et al* 2009, Jorgenson *et al* 2008, Lacelle *et al* 2010) creates an explicit need to quantify soil CO_2 emissions and study its governing controls within these features.

Here we use a space-for-time substitution that we refer to as a thaw slump 'chronosequence' to examine the evolution of soil CO_2 efflux before (undisturbed tundra), during (active thaw slump), and after (stabilized, revegetated thaw slump) formation of a large retrogressive thaw slump. In 2011 and 2012, we quantify soil CO_2 efflux during peak summer conditions and examine the importance of soil moisture, temperature, and soil physical properties in governing the release of CO_2 across the chronosequence.

2. Setting and study design

2.1. Site setting

The Selawik slump area is located along the upper Selawik River (157°36′43″W, 66°29′54″N) in northwestern Alaska (figure 1). This area is composed of an upland tussock shrub tundra community, an active retrogressive thaw slump that initiated in 2004, and a stabilized retrogressive thaw slump revegetated by a black spruce forest that is estimated to be >500 years old.

Mean annual precipitation for this area is 256 mm yr^{-1} and mean annual air temperature (MAAT) is −5.67 °C, averaged from >30 years of daily measurements at Kotzebue Airport, ∼130 miles east of the study area. The soil temperature regime is gelic, based on mean annual soil temperature at 50 cm < 2 °C as approximated from the MAAT at Kotzebue Airport. The soil moisture regime, as measured in July and early August, is classified as aquic based on the poorly drained condition gleyed soil color as observed in the field (Soil Survey Staff 2010). The parent material in this area is a glacial diamict composed of poorly sorted silt, gravel and cobble overlain by 2–5 m of fine-grained loess (Lanan 2013). Measured thaw depth in July and August varied between the different sites and extends to depths of 0.3–0.8 m. Because this field site is remote (∼108 km east of Selawik Village) and has limited access during spring, fall, and winter, our sampling was focused on summer months, when we expected to observe the highest CO_2 effluxes, due to higher temperatures and biologic activity.

2.2. Thaw slump chronosequence: a space for time substitution

We used a space for time substitution (thaw slump chronosequence) to examine changes in soil CO_2 efflux as a thaw slump evolves. The chronosequence includes three stages of feature evolution, with increasing maturity: undisturbed tundra, active slump, and stabilized slump (figure 1). Differences in vegetation between the three stages are a function of time since landform disturbance, and local environmental conditions. In this chronosequence conceptual model, the final state of the active slump will be similar in nature to the stabilized slump, due to common geomorphic and ecosystem drivers.

The tundra has not undergone any physical disturbance and represents the reference, or initial, condition. We sampled the tundra directly to the north of the Selawik slump headwall (figure 1), where the surface is relatively flat (sloping 1°–2° to the south). Primary vegetation consists of sedge and tussocks (*Eriophorum vaginatun, and Carex spp.*) with interspersed moss and lichen. Summer thaw depths ranges from 30 to 60 cm. Soil pits confirm that this soil is a Ruptic Histoturbel (Soil Survey Staff 2010), characterized by a wet, poorly decomposed, variably thick (15–20 cm) peat, that transitions to a fine-grained mineral soil with evidence of cryoturbation (figure 2(a)). These site characteristics (table 1) are consistent with findings from a recent regional survey (Jorgenson *et al* 2009).

The active retrogressive thaw slump, initiated in 2004, is one of only a handful of known active mega-slumps globally

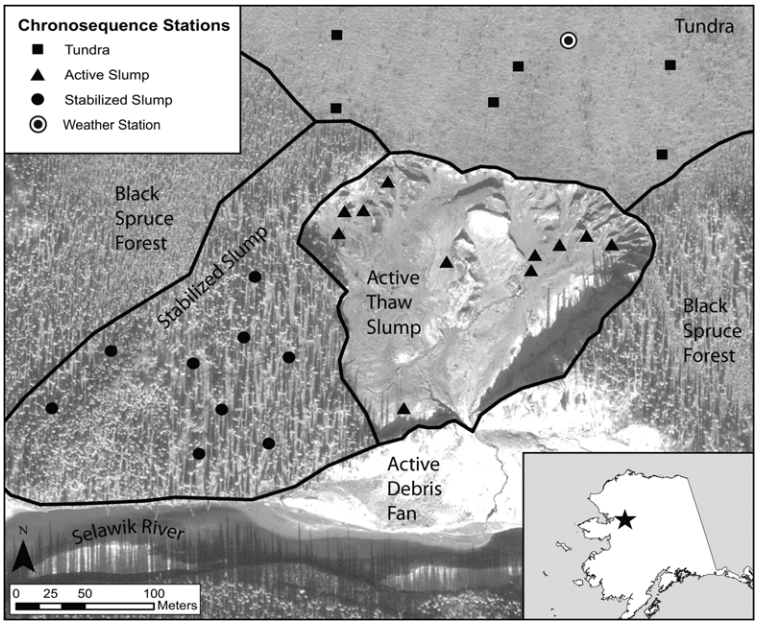

Figure 1. Map view of the Selawik slump showing boundaries of the chronosequence units and sampling sites within the tundra (squares), active slump (triangles), and stabilized slump (circles). The Selawik River flows east to west at the base of the image. The inlay map in the bottom right corner shows the location of the field area in Alaska. Location of the weather station used is denoted by a black circle with white ring.

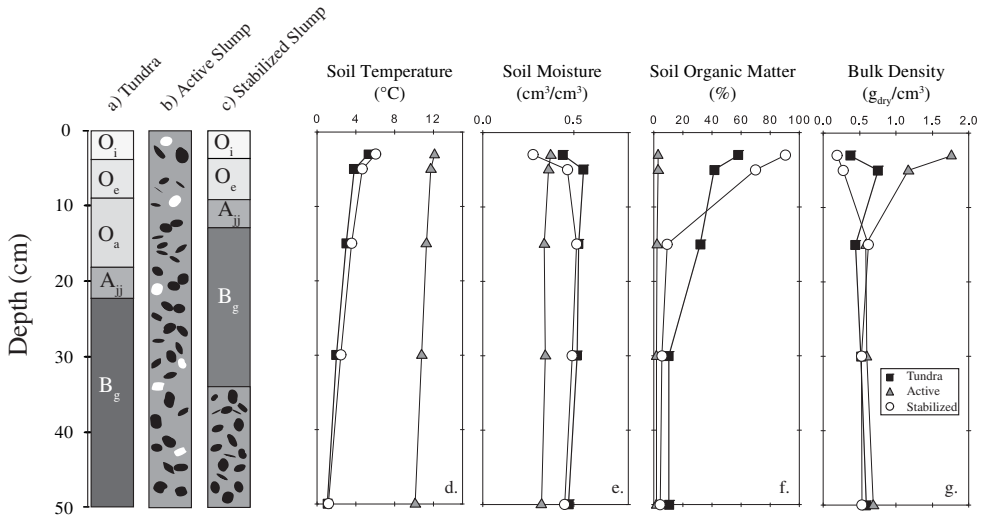

Figure 2. Schematic soil profiles for (a) tundra, (b) active slump, (c) stabilized slump, where O_i is comprised of fibrous materials from plant residue (least decomposed), O_e is partially decomposed organic matter, and O_a is highly decomposed (humified) organic matter. A_{jj} is cryoturbated humus-rich mineral horizon, and B_g is gleyed mineral horizon comprised of loess in tundra and material similar to the active slump and stabilized slump. Note that active slump material is mixed and cryoturbated loess (gray), peat (white) and coarse diamict (black) eroded from headwall, with fine-grained silts dominating the top 15 cm. Soil profiles for average (d) soil temperature, (e) soil moisture, (f) soil organic matter and (g) bulk density in for each of the three chronosequence stages. Note that the active slump develops very high bulk density in the upper portions of the soil.

(def. by Kokelj *et al* 2013). The slump has mobilized more than 0.5 M m^3 of ice and sediment, and expands at a rate of ~20 m yr^{-1} (Barnhart and Crosby 2013). The floor of the slump is ~50 000 m^2 (5 ha) and slopes at ~10°–25° toward the south. The vertical frozen headwall measures 15–18 m tall and is composed mostly of glacial diamict overlain by ~2–5 m of loess, with a 20 cm upper cap of organic-rich horizon and tussock community, as seen in the undisturbed tundra. The vast majority of the eroded material is diamict, and the active slump floor is largely composed of overlapping mudflows of unsorted silts and gravels. The upper 5–10 cm of the slump floor is characterized by finer-grained silts deposited

Table 1. Chronosequence characteristics. All parameters are averaged over the stations within each feature. Soil organic matter and bulk densities are for the top 8 cm of soil.

	Land cover type	Soil type	Average soil organic matter (%)	Average bulk density (g_{dry} cm^{-3})	July thaw depth (cm)	Slope (deg)
Tundra	Shrub, Sedge, Tussock, Moss, Lichen	Ruptic hisoturbels	58	0.4	30–60	2
Active slump	None. Bare mineral diamict, 3% — vegetated tundra rafts	Typic aqiturbels	3	1.8	>1 m	10–25
Stabilized slump	Black spruce, alder, grasses	Histic aquiturbels	91	0.2	50–80	10–25

through alluvial processes reworking thawed materials. The organic-rich horizon at the top of the headwall mixes into the slurry of thawed diamict following collapse (figure 2(b)). Because the organic material makes up such a small percentage of the total volume of material entering the slump, thus there is no organic horizon, the poorly drained loamy soils are classified as a Typic Aquiturbels (Jorgenson *et al* 2009, Soil Survey Staff 2010). A small portion (∼3%) of the slump floor is mantled by vegetated rafts (0.05–0.5 m^2 each), composed of intact pieces of tundra or peat that have detached from the headwall and are transported with sediment downslope. Frost probing revealed no permafrost in the upper meter of the slump floor (table 1).

The stabilized slump is directly adjacent to and west of the active slump (figure 1), and also slopes at 10°–25° toward the south. The stabilized slump represents a likely evolutionary trajectory for the active thaw slump. Following catastrophic slumping, the sharp edges of the stabilized feature diffused away and the surface has been recolonized by black spruce, alder (*Piceamariana and Alnus spp*.), and various grasses. Soils developed on the slump material have ∼10 cm of accumulated organic matter above the loamy, poorly drained and cryoturbated mineral soil with fine roots Jorgenson *et al* (2009). These soils are classified as Histic Aquiturbels (figure 2(c); Soil Survey Staff 2010). Summer thaw depths range from 50–80 cm (table 1). The feature is thought to be >500 years old based on the presence of numerous generations of black spruce logs found decaying on the surface.

3. Methods

3.1. Meteorology

During our study, continuous air temperature and precipitation were collected in thirty minute intervals from a weather station located in undisturbed tundra ∼10 m north of the active slump headwall (figure 1). Air temperature was collected using a shielded sensor 215 cm above ground and precipitation was collected using a tipping-bucket 242 cm above ground. Data were collected from January to September in 2011, and from June to early December in 2012. Due to the close proximity of the chronosequence to the weather station, and previous studies of thaw slump microclimate (Grom and Pollard 2008), we treat precipitation and air temperature data as consistent across three stages.

3.2. Point measurements of CO_2 efflux, soil temperature, soil moisture

Twenty six sampling sites for soil CO_2 efflux, soil temperature, and soil moisture were established along our defined chronosequence (figure 1). Sites within a given stage of the chronosequence were deliberately chosen to include different types of vegetation to assess heterogeneity within each stage. In July 2011, each site was sampled ∼5 times during a six-day sampling period. In July–August 2012, each site was sampled ∼12 times over an eighteen-day sampling period. Sampling times for each collar were irregularly distributed through the day and night to account for possible temporal variability in environmental parameters.

To measure soil CO_2 efflux (defined to include CO_2 generated below ground by multiple processes, predominantly microbial and root respiration), above-ground vegetation was removed by clipping, a 10.2 cm diameter polyvinyl chloride pipe (soil collar) was driven ∼8 cm into the upper portion of the soil column, and the soil was allowed to stabilize for twenty-four hours prior to any measurements (LI-COR 2007). Soil CO_2 efflux was measured using a LiCor-8100A analyzer (Lincoln, NE) fitted to a LiCor-8100-102 10 cm diameter survey chamber with a volume of 854.2 cm^3. The survey chamber was placed on top of the soil collar and set to a 1.5 min measuring interval. In 2012, after measuring efflux, soil pits were dug to 60 cm depth and soils were described using standard soil survey methods (Schoenberger *et al* 2002). Soil temperature was measured at depths of 3, 5, 15, 30 and 50 cm depth with a LiCor-8100-203 soil thermistor probe. Volumetric water content (VWC), hereafter referred to as soil moisture, was measured at the same depths using a Delta-T ML2x probe. Post-processing of soil CO_2, temperature and soil moisture was conducted using the LI-8100 data file viewer (v2.0). Soil volumetric water content was adjusted for high organic content soils using the equation provided in the LI-COR manual (2007).

3.3. Physical and chemical soil properties

In 2012, soil bulk density and soil organic matter content were determined for a subset of sites along the chronosequence. After flux measurements were taken, soil samples of known volume were excised from the soil collar and pits at depths of 3, 5, 15, 30 and 50 cm, frozen and transported back to Idaho State University, where they were analyzed for soil organic matter (SOM) content and bulk density following methods described by (Schumacher 2002, Blake and Hartge 1986), respectively. In brief, SOM was determined by loss-on-ignition by combusting 100 g of dry soil for 24 h at 500 °C and reweighing the weight loss. Bulk density was determined by drying the soil at 105 °C for 24 h to weigh the dry mass and corrected for the volume of rock fragments if present.

3.4. Statistical analysis

Repeated soil CO_2, soil temperature and moisture measurements were averaged for each sampling location. CO_2 efflux measurements were log transformed to improve normality and homoscedasticity Other parameters such as soil moisture and soil temperature were normally distributed and thus did not require transformation. ANOVA and Tukey-Kramer HSD statistical tests for soil CO_2 efflux, soil temperature, and soil moisture were used to determine statistical differences within each stage (tundra, active, and stabilized slump) along the chronosequence. Sampling locations within each stage showed no significant differences allowing data from each stage to be pooled for both 2011 and 2012. ANOVA tests and Tukey-Kramer HSD were then conducted to determine statistical differences between parameters measured in each chronosequence stages during 2011 and 2012. Linear and multiple linear regression models were used to determine environmental controls on soil CO_2 efflux. All statistical analyses were performed in JMP 10 (Cary, NC) software.

4. Environmental conditions over space and time

Soil CO_2 efflux is a function of both above- and below-ground environmental conditions that vary over time, as well as in response to the physical characteristics of the soil itself, and the type of vegetation living in and above it. In this section, we describe the variability in these parameters during the two years of our investigation. The implications of environmental variability, as well as variability in key soil physical characteristics on soil CO_2 efflux are discussed in a following section.

4.1. Precipitation

Both the magnitude and intensity of precipitation were higher during the 2012 campaign than in 2011. Cumulative precipitation during the 2011 sampling period (figure 3(a)) increased due to two small events totaling 9 mm. In contrast, the 2012 sampling period included three significant events, the first of which delivered 20 mm early in the campaign, with subsequent events in the latter half of the campaign delivering ∼5 mm each.

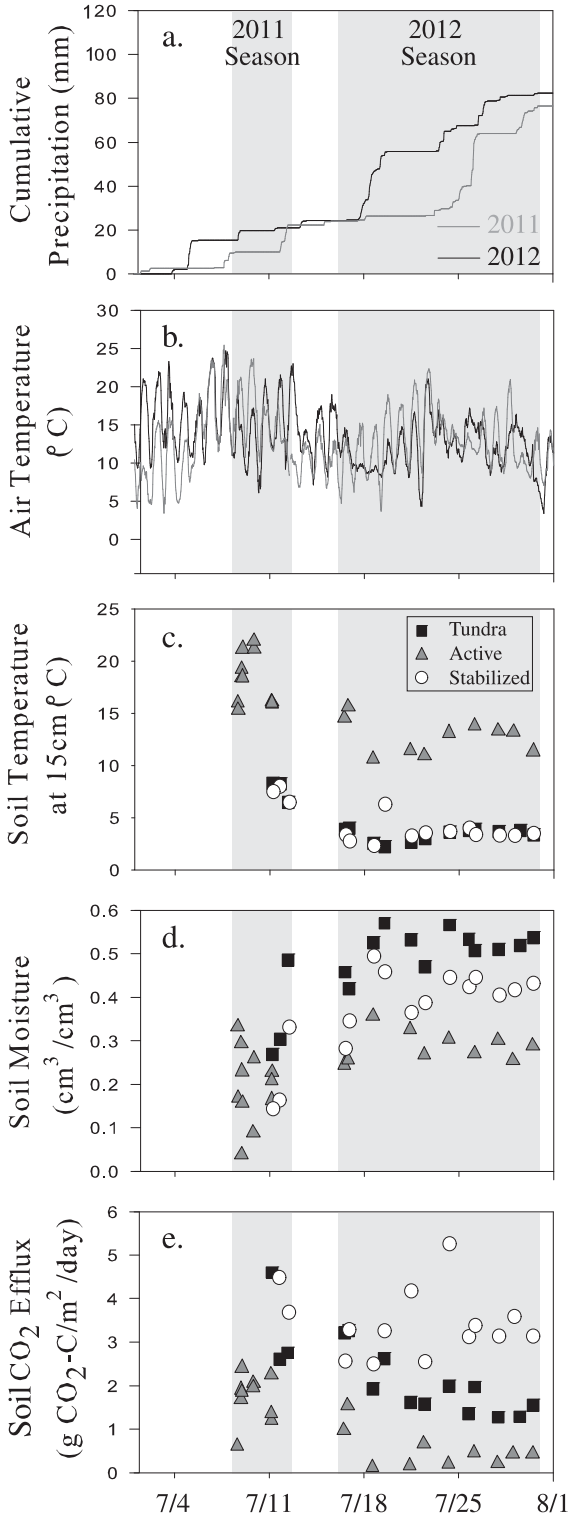

Figure 3. Day-of-the-year time series of environmental variables for 2011 and 2012 field seasons (shaded regions). Plots show (a) cumulative precipitation (mm), (b) air temperature (°C), (c) soil temperature at 15 cm (°C), (d) soil moisture at 10 cm (cm^3/cm^3), (e) soil CO_2 efflux (g CO_2–C m^{-2} d^{-1}). For (a) and (b), gray and black lines represent local weather station data from 2011 and 2012 respectively. For (c)–(e), means are shown as black squares for tundra, gray triangles for the active slump, and white circles for the stabilized slump.

4.2. Air temperature

Air temperature was generally higher during the 2011 than the 2012 sampling period (figure 3(b)). Average air temperature during the 2011 sampling period was ∼16 °C, and showed an overall cooling trend. In contrast, 2012 average air temperature was lower, ∼14 °C, and showed a slight warming trend in the first half of the sampling period, followed by a slight cooling trend through the latter half of the period. For both 2011 and 2012, precipitation events corresponded to a considerable reduction in the magnitude of the diel cycle in air temperature.

4.3. Soil temperature

Average daily soil temperatures at 15 cm were consistently higher in 2011, for all three chronosequence stages (figure 3(c)). Soil temperatures at 15 cm were significantly different (figure 4(a)) between the three chronosequence stages for both 2011 and 2012 (2011 $F_{2,21} = 64.07$, $p < 0.0001$; 2012 $F_{2,25} = 78.4$, $p = 0.0001$). Post-hoc Tukey tests showed no significant differences between soil temperatures in the tundra and the stabilized slump features, however, active slump soil temperatures were significantly elevated by comparison (3–4 times higher in both 2011 and 2012 ($p < 0.05$)). We attribute higher active slump temperatures to the higher thermal conductivity and lower albedo of the dark, bare mineral soil in the active slump. The dense vegetation on the tundra and stabilized slump insulate the soil and shade it from solar radiation, dampening drastic changes in soil temperature. The tundra and stabilized slump also have shallower thaw depths, maintaining permafrost closer to the surface and, thus, lower soil temperatures. Temporal variations in soil temperatures at 15 cm show cooling in response to precipitation events in 2011 and 2012 (figure 3(c)). In 2012, average soil temperatures within each chronosequence stage decreased with and the profiles remained distinct from one another across the range of depths measured (figure 2(d)).

4.4. Soil moisture content

Average daily soil moisture at 15 cm depth were temporally more variable than soil temperatures, with generally higher soil moistures observed in 2012 than 2011 (figure 3(d)). In both years, soil moisture increased significantly following periods of precipitation. Average soil moisture at 15 cm differed significantly among chronosequence stages (figure 4(b)) with the tundra having higher soil moisture than the other two environments (2011 $F_{2,21} = 7.52$, $p < 0.0039$; 2012 $F_{2,25} = 5.08$, $p = 0.015$). Post-hoc Tukey tests revealed no significant differences between the active and the stabilized slump whereas soil moisture in tundra was significantly elevated relative to the other two stages ($p < 0.05$). Soil moisture was largely constant through the soil profiles when sampled in 2012 (figure 2(e)), decreasing slightly in the upper 5 cm of the tundra and stabilized slump.

We attribute the differences between the tundra and the active or stabilized slumps to differences in topographic setting. The tundra consists mostly of mosses, lichen and tussock communities on a slightly sloping surface, increasing water

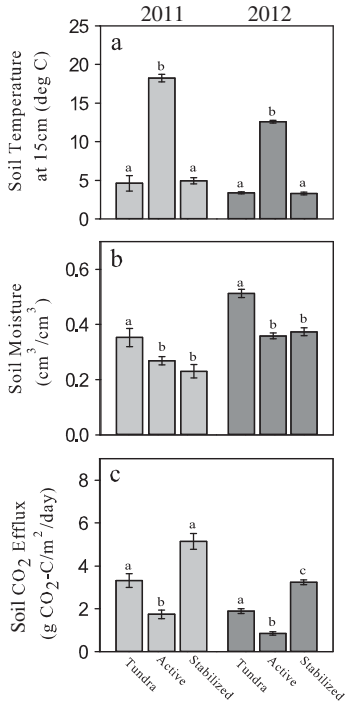

Figure 4. Growing season mean (a) soil temperature at 15 cm (°C), (b) soil moisture at 10 cm (cm^3/cm^3), and (c) soil CO_2 effluxes (g CO_2–C m^{-2} d^{-1}) in both 2011 (light gray) and 2012 (dark gray) for the tundra, active slump and stabilized slump. Bars represent the mean of all field season measurements and error bars represent one standard error. Letters above each bar represent the results for significant differences within year and across stages using a Tukey–Kramer HSD. Columns with similar letters are not significantly different.

residence times. In contrast, both the active and stabilized slumps are located on steeper surfaces, dipping 10°–25° toward the Selawik River, which should drain faster, reducing soil moisture. Alternatively, differences in soil organic matter and bulk density affect soil water holding capacity and could influence moisture contents across the three stages.

4.5. Soil properties

At depths below ∼20 cm, the soil organic matter (SOM) is low in all stages of the chronosequence (figure 2(f)). But, the upper portions of the soil profiles vary significantly, with values remaining <5% in the active slump, increasing upwards to 20–90% in the tundra, and increasing more consistently in the stabilized slump to values of 85–95% (figure 2(f); table 1). Elevated SOM contents in the upper portions of tundra and stabilized slump soils mark the transition to the cryoturbated soil A horizons, in each case reflecting accumulation of litter and the presence of active vegetation. As noted previously, the active slump dilutes the contribution from the 20 cm upper organic-rich horizon by mixing it with ∼15 m of loess and diamict. Despite the infrequent presence of vegetated rafts of organic-rich soils on the slump floor, their contribution does not appreciably enrich the materials on the active slump floor with SOM.

Bulk density profiles in the chronosequence soils were similar below ∼15 cm (∼0.6 g cm^{-3}), and diverged sig-

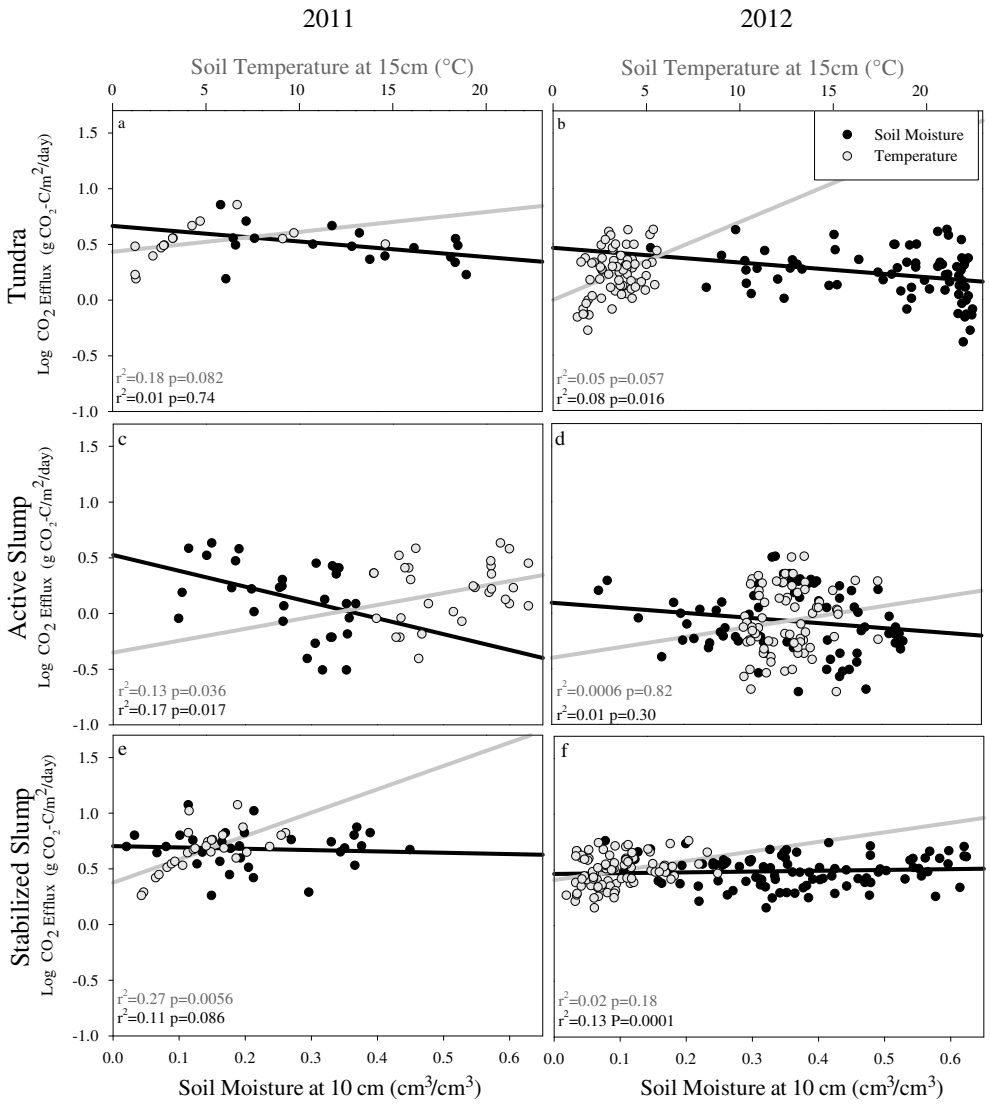

Figure 5. Correlations of soil CO_2 efflux (g CO_2–C m^{-2} d^{-1}) with soil temperature at 15 cm (°C) and soil moisture at 10 cm (cm^3/cm^3) in 2011 ((a), (c), (e)) and 2012 ((b), (d), (f)), within the chronosequence stages. For all graphs, regressions of soil moisture with soil CO_2 efflux are represented by black lines. Regressions of soil temperature with soil CO_2 efflux are represented by gray lines. r^2 and p values for each regression are given in each lower left corner.

nificantly in the upper 10 cm, with soils in the tundra and stabilized slump tending towards lower values of bulk density and soils in the active slump tending towards much higher values (figure 2(g)). Bulk densities at 8 cm depth are 0.6–0.8 g cm^{-3} in the tundra, 0.1–0.3 g cm^{-3} in the stabilized slump, and 1.3–2.2 g cm^{-3} in the active slump (table 1). The predominance of SOM in the upper portions of tundra and stabilized slump soils explains their lower bulk densities. Increased bulk density in the upper active slump profiles results when thawed sediment is remobilized and flows away from the headwall as a thick, viscous slurry, capping the slump floor with silts and clays.

4.6. Vegetation

Differing types of vegetation cover are present in the chronosequence stages. The active slump has no vegetation cover, the tundra is composed of mostly tussocks, sage, mosses and lichen, and the stabilized slump consists of black spruce, alder and various grasses. Studies of root respiration in Arctic ecosystems have estimated that up to 56% of soil CO_2 efflux in black spruce forests and up to 30% in tundra ecosystems which can be attributed to fine root respiration (Raich and Schlesinger 1992, Ruess *et al* 2003). We therefore expect that the soil CO_2 effluxes in these chronosequence stages are influenced to a different degree by root respiration. In the unvegetated active slump root respiration is negligible. For both 2011 and 2012, the type and extent of vegetation did not change within the three environments and therefore influences of vegetation are consistent between study years.

5. CO_2 efflux over space and time

Average peak growing season soil CO_2 efflux in the different chronosequence stages and field seasons are summarized in figure 4 and table 2, along with average soil temperature

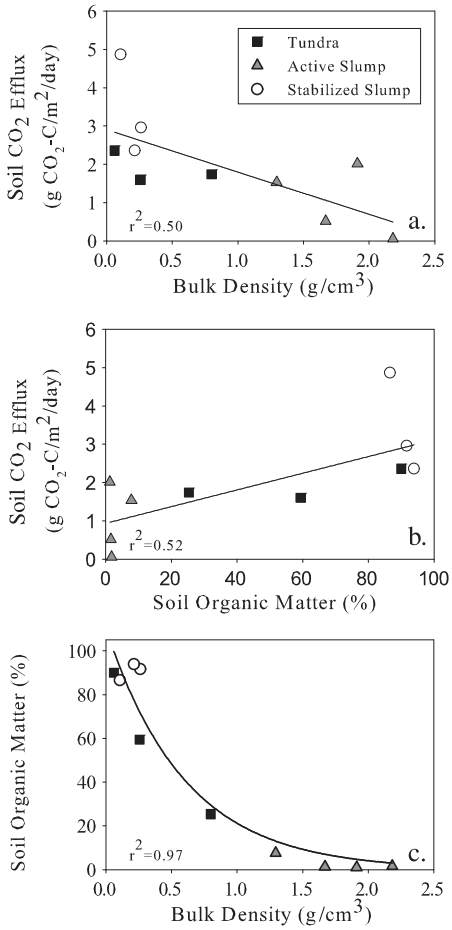

Figure 6. (a) Negative linear correlation between bulk density (g cm^{-3}) and soil CO_2 efflux (g CO_2–C m^{-2} d^{-1}). (b) Positive linear correlation between soil organic matter (%) and soil C_O2 efflux (g CO_2–C $m^{-2}d^{-1}$). (c) Negative exponential correlation between soil organic matter (%) and bulk density (g cm^{-3}) in the first 8 cm of soil. For all graphs, chronosequence stages are represented as follows: tundra *(black squares)*, active slump *(gray triangles)*, stabilized slump *(white circles)*.

and soil moisture values. Soil CO_2 effluxes were significantly different among the chronosequence stages (figure 4(c)) and differed between years (2011, $F_{3,22} = 12.69$ $p < 0.0001$, 2012 $F_{3,25} = 27.48$, $p < 0.0001$). In 2011, soil CO_2 efflux from the tundra and stabilized slump were similar and fluxes from the active slump were significantly lower ($p < 0.05$). Conversely, in 2012, the soil CO_2 effluxes from all stages were significantly different from each other, with the highest effluxes from the stabilized slump and lowest from the active slump.

Measurements of soil CO_2 efflux were scaled up to estimate the total amounts of carbon lost to the atmosphere per day during peak growing season (table 2). Numerous studies have determined the average carbon released from the tundra as CO_2 during the growing season at more northerly locations (Giblin *et al* 1991, Poole and Miller 1982, Raich and Schlesinger 1992). Our observed effluxes are 1.5–2 times higher, potentially due to the dampening effect of cooler temperatures their the more northerly field areas. Average carbon released from CO_2 in the active slump during peak summer in 2011 was 1.75 ± 0.15 g CO_2–Cm^{-2} d^{-1} (table 2). In 2012, the amount was half as large (0.86 ± 0.24 g CO_2–C m^{-2} d^{-1}). These values fall within the lower range of soil CO_2 efflux measured along a gradient of minimally- to extensively-thawed, fully-vegetated, low gradient and gradually-thawed thermokarst sites in central Alaska (Lee *et al* 2010, Schuur *et al* 2009) (table 2). Unlike our system, these sites did not experience thermal erosion, but maintained their soil structure as the frost table deepened, allowing for more carbon to become functionally available. Compared to our site, albedo changes along the gradual thaw gradient were insignificant. The values that we observed for soil CO_2 efflux in the active slump were similar to the minimal-thaw sites reported in these studies. Average soil carbon released from the stabilized slump was 5.14 ± 0.27 g CO_2–C m^{-2} d^{-1} during peak summer 2011, and 3.24 ± 0.13 g CO_2–C m^{-2} d^{-1} during 2012. These measurements fall within in the higher range of soil CO_2 efflux measurements reported for Alaskan black spruce forests (Raich and Schlesinger 1992, Schlentner and van Cleve 1985, Vogel *et al* 2008) (table 2). But, we note that values reported in other studies averaged measurements over the full year, while values in this study are calculated only for the peak growing season, which would tend to be larger than annual averages.

5.1. Controls affecting CO_2 efflux

5.1.1. Soil temperature and moisture. Relationships between soil temperature or moisture and soil CO_2 efflux are examined in figure 5. We see that soil moisture exerts a slightly stronger control on soil CO_2 efflux in 2011, but, in 2012, soil temperature appears to be slightly more important. We suggest that, during the warmer and drier 2011season, our system was water-limited, and therefore soil moisture exerted a stronger control on soil CO_2 efflux. In 2012, due to the increased precipitation, the system was no longer water limited and soil temperature exerted stronger control on soil CO_2 efflux.

The weak correlations between soil temperature or moisture and soil CO_2 efflux in the Selawik chronosequence is likely due, in part, to limited environmental variation during our sampling campaign. If we had been able to collect data in the shoulder seasons, we believe that we would have observed higher correlations between soil temperature and moisture with soil CO_2 efflux. Also, although we measured soil CO_2 efflux intermittently during both day and night, we did not use automated chambers to collect efflux and soil conditions at regular, high frequency intervals. Because measurements were made at irregular times over multiple days, when environmental conditions were also changing, we have less explanatory power. For example, one measurement might have been made on a warm, dry night and another on a cool, dry night.

In general, our results show that soil CO_2 efflux increased with increasing soil temperature, and decreased with increasing soil moisture, as similarly reported for Arctic soils (Michaelson and Ping 2003, Oberbauer *et al* 2007). Yet, these correlations are unexpectedly weak (R^2 all less than 0.27), even if most the signs of the correlations between variables were consistent with the observations of other workers (Huemmrich *et al* 2010, Michaelson and Ping 2003, Natali *et al* 2011, Oberbauer *et al* 2007, Peterson and Billings 1975).

Table 2. Average daily CO_2 efflux (g CO_2–C m^{-2} d^{-1}) in 2011 and 2012 for each chronosequence stage. Comparable CO_2 effluxes reported in literature.

	2011 CO_2 efflu (g–CO_2–C m^{-2} d^{-1})	2012 CO_2 efflu (g–CO_2–C m^{-2} d^{-1})	Comparable CO_2 efflux (g–CO_2–C m^{-2} d^{-1}
Tundra	3.32 ± 0.027	1.89 ± 0.16	0.46–1.7[a,b,c]
Active slump	1.75 ± 0.15	0.86 ± 0.23	0.72–2.64[d,e]
Stabilized slump	5.14 ± 0.27	3.24 ± 0.13	0.264–5.89[f,g,h]

[a] Giblin *et al* (1991). [b] Poole and Miller (1982). [c] Raich and Schlesinger (1992). [d] Lee *et al* (2010). [e] Schuur *et al* (2009). [f] Raich and Schlesinger (1992). [g] Schlentner and van Cleve (1985). [h] Vogel *et al* (2008).

5.1.2. Soil properties. In contrast to the weak correlations with soil moisture and temperature, soil CO_2 efflux correlates strongly with soil properties, such as a strong inverse correlation between bulk density ($R^2 = 0.50$) (figure 6(a)). Within the chronosequence, the tundra and stabilized slump have the lowest bulk densities and highest average soil CO_2 effluxes (tables 1 and 2), whereas the active slump has the highest bulk densities and lowest soil CO_2 effluxes (figure 6(a)). Indeed, soil bulk density values in the active slump approached typical particle density values of $\sim$2.2 g cm^{-3}. These findings suggest that higher bulk densities may provide a diffusion limitation in the active slump, possibly inhibiting gas from exchanging with the surface (Davidson and Trumbore 1995).

We found a strong positive correlation between soil organic matter and soil CO_2 efflux ($R^2 = 0.51$) (figure 6(b)). The tundra and stabilized slump had the highest SOM and highest soil CO_2 efflux, while the active slump had the lowest soil SOM content and the lowest soil CO_2 efflux. This suggests an organic substrate contributing to CO_2 production and efflux. Though our measurements of soil CO_2 efflux do not distinguish between root respiration and microbial respiration, we expect that rates of root respiration and SOM would present similar correlations with soil CO_2 efflux. The lack of vegetation on the active slump floor should play a significant role in reducing the CO_2 efflux relative to the tundra or stabilized slump, which contain extensive networks of fine roots. Our results suggest that soil physical and chemical properties, such as bulk density and SOM, more strongly influence soil CO_2 efflux than environmental factors such as soil temperature and moisture. Previous studies suggest that the primary control on CO_2 efflux is % SOM (Alexander 1989, Michaelson and Ping 2003). Although we cannot differentiate whether SOM or bulk density is more influential in controlling CO_2 efflux in our study area (because of the strong inverse correlation between SOM and bulk density (figure 6(c))), these observations suggest fruitful avenues for future thaw slump studies.

6. Implications and conclusions

In a warming Arctic, the prevalence of thaw slumps and, in particular, very large, rapidly evolving features such as the Selawik thaw slump, are predicted to increase in frequency (Gooseff *et al* 2009, Lacelle *et al* 2010, Rowland *et al* 2010). This study contributes to our knowledge of how these retrogressive thaw slumps evolve over time and give rise to changes in soil physical and chemical properties that either limit or enhance soil CO_2 efflux. While previous studies have shown strong correlations between soil CO_2 efflux and soil temperature or moisture, the present study suggests that physical and chemical soil properties, such as bulk density and SOM content, may also be important controls on soil CO_2 efflux.

Findings from this study indicate that quantifying the initial quantity of organic substrate, used as a proxy for carbon availability, as well as the material's diffusivity will likely be of great importance to understanding soil CO_2 efflux in these rapidly changing environments. The Arctic is composed of a heterogeneous landscape where substrate soil organic matter ranges from 1–3%, as seen at the active Selawik slump, to >78%, as seen in yedoma soils of northern Alaska and Siberia (Kanevskiy *et al* 2011). Future studies will need to assess seasonal fluxes across these features and determine controls governing soil CO_2 efflux in thermal erosion features developed in materials with higher organic content.

Our research also suggests that geomorphic controls governing the initiation and development of thaw slumps influence overall soil CO_2 efflux. Hillslope thermokarst features such as retrogressive thaw slumps may cause compaction, mixing and erosion of soils, decreasing soil organic content, and increasing soil bulk density. Thus, despite very rapid warming of the permafrost during formation of large thermal erosion features, and the potential for rapid release of permafrost carbon to the atmosphere, soil structural changes, in fact, appear to reduce soil CO_2 emissions due to diffusivity limitations and erosion of organic-rich soil horizons, and merit further study.

Acknowledgments

This research received financial and logistic support from the Institute of Geophysics and Planetary Physics at Los Alamos National Laboratory (LANL IGPP Minigrant 166259), the Selawik National Wildlife Refuge (USFWS – CESU 84320-9-J306R) as well as financial support from the NSF's Arctic System Science (ARCSS) Program (OPP – 0806399) and the NSF Idaho EPSCoR Program in Water Resources in a Changing Climate (EPS 0814387). Benjamin Abbott provided inspiration, guidance and feedback for the study design, methods and interpretation. Meteorological data were provided by Joel Rowland of LANL. The authors thank Tina Moran, Theo Barnhart, Pat Calhoun, Kelsey Lanan and Joel Rowland for field and logistical support. Reviews from Keith Reinhart and three anonymous reviewers significantly improved manuscript quality and readability.

References

Alexander E B 1989 Bulk density equations for southern Alaska soils *Can. J. Soil Sci.* **69** 177–80

Arctic Climate Impact Assessment 2004 *Impacts of a Warming Climate: Arctic Climate Impact Assessment Overview Report* (New York: Cambridge University Press)

Barnhart T B and Crosby B T 2013 Comparing two methods of surface change detection on an evolving thermokarst using high-temporal-frequency terrestrial laser scanning, Selawik River, Alaska *Remote Sens.* **5** 2813–23937

Blake G R and Hartge G E 1986 *Bulk Density* in *Methods of Soil Analysis Part 1—Physical and Mineralogical Methods (Agronomy Monograph no. 9)* ed A Klute (Madison, WI: American Society of Agronomy) pp 363–75

Davidson E A and Trumbore S E 1995 Gas diffusivity and production of CO_2 in deep soils of the eastern Amazon *Tellus* B **47** 550–65

Duarte C M, Lenton T M, Wadhams P and Wassmann P 2012 Abrupt climate change in the Arctic *Nature Clim. Change* **2** 60–2

Giblin A E, Nadelhoffer K J, Shaver G R, Laundre J A and McKerrow A J 1991 Biogeochemical diversity along a riverside toposequence in arctic Alaska *Ecol. Monograph.* **61** 415–35

Gooseff M N, Balser A, Bowden W B and Jones J B 2009 Effects of hillslope thermokarst in northern Alaska *Eos Trans. AGU* **90** 29

Grom J D and Pollard W H 2008 A study of high Arctic retrogressive thaw slump dynamics, Eureka Sound Lowlands, Ellesmere Island *Proc. 9th Int. Conf. on Permafrost* vol 29

Grosse G *et al* 2011 Vulnerability of high-latitude soil organic carbon in North America to disturbance *J. Geophys. Res.* **116** (G4) G00K06

Hinzman L *et al* 2005 Evidence and implications of recent climate change in northern Alaska and other arctic regions *Clim. Change* **72** 251–98

Huemmrich K F, Kinoshita G, Gamon J A, Houston S, Kwon H and Oechel W C 2010 Tundra carbon balance under varying temperature and moisture regimes *J. Geophys. Res.: Biogeosci. (2005–2012)* **115** (G4)

IPCC 2007 *Climate Change 2007: Synthesis Report. Contribution of Working Groups I, II and III to the Fourth Assessment Report of the Intergovernmental Panel on Climate Change* vol 446 (New York: Cambridge University Press) 104 p

Jorgenson M T and Osterkamp T E 2005 Response of boreal ecosystems to varying modes of permafrost degradation *Can. J. Forest Res.* **35** 2100–11

Jorgenson M T, Romanovsky V, Harden J, Shur Y, O'Donnell J, Schuur E A G, Kanevskiy M and Marchenko S 2010 Resilience and vulnerability of permafrost to climate change *Can. J. Forest Res.* **40** 1219–36

Jorgenson M T, Roth J E, Miller P F, Macander M J, Duffy M S, Wells A F, Frost G V and Pullman E R 2009 *An ecological land survey and landcover map of the Selawik National Wildlife Refuge, ABR, Inc. and US Fish and Wildlife Service* 251p (available at: http://permafrost.gi.alaska.edu/sites/default/files/Selawik%20ELS_Nov09_FINAL.pdf)

Jorgenson M T, Shur Y L and Osterkamp T E 2008 *Thermokarst in Alaska, 9th Int. Conf. on Permafrost* vol 29 pp 869–76

Jorgenson M T, Shur Y L and Pullman E R 2006 Abrupt increase in permafrost degradation in Arctic Alaska *Geophys. Res. Lett.* **33** L02503

Kanevskiy M, Shur Y, Fortier D, Jorgenson M T and Stephani E 2011 Cryostratigraphy of late pleistocene syngenetic permafrost (yedoma) in northern Alaska, Itkillik river exposure *Quat. Res.* **75** 584–96

Kokelj S V and Jorgenson M T 2013 Advances in thermokarst research *Permafrost Periglacial Process.* **24** 108–19

Kokelj S V, Lacelle D, Lantz T C, Tunnicliffe J, Malone L, Clark I D and Chin K S 2013 Thawing of massive ground ice in mega slumps drives increases in stream sediment and solute flux across a range of watershed scales *J. Geophys. Res.* **118** 681–92

Koven C D, Ringeval B, Friedlingstein P, Ciais P, Cadule P, Khvorostyanov D and Tarnocai C 2011 Permafrost carbon-climate feedbacks accelerate global warming *Proc. Natl Acad. Sci.* **108** 14769–74

Lacelle D, Bjornson J and Lauriol B 2010 Climatic and geomorphic factors affecting contemporary (1950–2004) activity of retrogressive thaw slumps on the Aklavik Plateau, Richardson Mountains, NWT, Canada *Permafrost Periglacial Process.* **21** 1–15

Lanan K M 2013 Glacial and geomorphic history of the upper Selawik valley, northwestern Alaska, with implications for thermokarst formation *MS Thesis* Idaho State University

Lantz T C and Kokelj S V 2008 Increasing rates of retrogressive thaw slump activity in the Mackenzie Delta region, N.W.T. Canada *Geophys. Res. Lett.* **35** L06502

Lawrence D M, Slater A G, Tomas R A, Holland M M and Deser C 2008 Accelerated Arctic land warming and permafrost degradation during rapid sea ice loss *Geophys. Res. Lett.* **35** L11506

Lee H, Schuur E, Vogel J and Lavoie M 2011 A spatially explicit analysis to extrapolate carbon fluxes in upland tundra where permafrost is thawing *Glob. Change Biol.* 1379–93

Lee H, Schuur E A G and Vogel J G 2010 Soil CO_2 production in upland tundra where permafrost is thawing *J. Geophys. Res.: Biogeosci. 2005–2012* **115** (G1)

LI-COR 2007 *LI-8100 Automated Soil* CO_2 *Flux System and LI-8150 Multiplexer Instruction Manual* (Lincoln: LI-COR Inc.)

Michaelson G J and Ping C L 2003 Soil organic carbon and CO_2 respiration at subzero temperature in soils of arctic Alaska *J. Geophys. Res.* **108** 8164

Natali S M, Schuur E A G, Trucco C, Hicks Pries C E, Crummer K G and Baron Lopez A F 2011 Effects of experimental warming of air, soil and permafrost on carbon balance in Alaskan tundra *Glob. Change Biol.* **17** 1394–407

Oberbauer S F, Tweedie C E, Welker J M, Fahnestock J T, Henry G H R, Webber P J, Hollister R D, Walker M D, Kuchy A, Elmore E and Starr G 2007 Tundra CO_2 fluxes in response to experimental warming across latitudinal and moisture gradients *Ecol. Monographs* **77** 221–38

Peterson K M and Billings W D 1975 Carbon dioxide flux from tundra soils and vegetation as related to temperature at barrow, Alaska *Am. Midland Naturalist* **94** 88–98

Poole D K and Miller P C 1982 Carbon dioxide flux from three arctic tundra types in north-central Alaska, USA *Arctic Alpine Res.* **14** 6

Raich J W and Schlesinger W H 1992 The global carbon dioxide flux in soil respiration and its relationship to vegetation and climate *Tellus* B **44** 81–99

Ruess R W, Henderick R L, Burton A J, Pregitzer K S, Sveinbjornsson B, Allen M F and Maurer G E 2003 Coupling fine root dynamics with ecosystem carbon sycling in black spruce forests of interior Alaska *Ecol. Monographs* **73** 643–62

Rowland J C *et al* 2010 Arctic landscapes in transition: responses to thawing permafrost *Eos Trans. AGU* **91** 229–30

Schlentner R E and van Cleve K 1985 Relationships between CO_2 evolution from soil, substrate temperature, and substrate moisture in four mature forest types in interior Alaska *Can. J. Forest Res.* **15** 10

Schoenberger P J, Wysocki D A, Benham E C and Broderosn W D 2002 *Field Book for Describing and Sampling Soils* version 2.0 (Lincoln, NE: National Soil Survey Center)

Schumacher B A 2002 Methods for the determination of total organic carbon (TOC) in soils and sediments *National ESD* ed EPA

Schuur E and Abbott B 2011 High risk of permafrost thaw *Nature* **480** 32–3

Schuur E A G *et al* 2008 Vulnerability of permafrost carbon to climate change: implications for the global carbon cycle *BioScience* **58** 701–14

Schuur E A G, Vogel J G, Crummer K G, Lee H, Sickman J O and Osterkamp T E 2009 The effect of permafrost thaw on old carbon release and net carbon exchange from tundra *Nature* **459** 556–9

Soil Survey Staff 2010 *Keys to Soil Taxonomy* vol 11 (Washington, DC: Pocahontas Press)

Tarnocai C, Canadell J G, Schuur E A G, Kuhry P, Mazhitova G and Zimov S 2009 Soil organic carbon pools in the northern circumpolar permafrost region *Global Biogeochem. Cycles* **23** 1–11

Vogel J, Schuur E A, Trucco C and Lee H 2009 Response of CO_2 exchange in a tussock tundra ecosystem to permafrost thaw and thermokarst development *J. Geophys. Res.: Biogeosci. (2005–2012)* **114** (G4)

Vogel J G, Bond-Lamberty B P, Schuur E A G, Gower S T, Mack M C, O'Connell K E B, Valentine D W and Ruess R W 2008 Carbon allocation in boreal black spruce forests across regions varying in soil temperature and precipitation *Glob. Change Biol.* **14** 1503–16

Winton M 2006 Amplified Arctic climate change: what does surface albedo feedback have to do with it? *Geophys. Res. Lett.* **33** L03701